Journal of Magnetic Resonance **141,** 335–339 (1999)
Article ID jmre.1999.1894, available online at http://www.idealibrary.com on IDEAL®

COMMUNICATIONS

Probing Membrane Surfaces and the Location of Membrane-Embedded Peptides by ^{13}C MAS NMR Using Lanthanide Ions

Gerhard Gröbner,[1] Clemens Glaubitz, and Anthony Watts

Biomembrane Structure Unit, Department of Biochemistry, University of Oxford, South Parks Road, Oxford OX1 3QU, United Kingdom

E-mail: gerhard@bioch.ox.ac.uk

Received February 8, 1999; revised April 9, 1999

A simple but efficient ^{13}C MAS NMR method is presented for the determination of the location of embedded molecules such as peptides relative to biological membrane surfaces by exploiting the interaction with paramagnetic lanthanide ions. Using various aqueous Dy^{3+} concentrations a distance-dependent differential paramagnetic quenching of NMR lipid resonance intensities for specific carbon sites was observed, with residues at the bilayer surface quenched effectively and hydrophobic sites unaffected by Dy^{3+}. Tested on the membrane-embedded 50 residue long M13 coat protein, ^{13}C labeled at its Val-29 and Val-31 residues, no paramagnetic quenching was observed for the peptide resonances by Dy^{3+}, suggesting that Val-29 and Val-31 are not in close proximity to the bilayer interface, but buried deeply inside the hydrophobic region of the lipid bilayer.

Key Words: **membranes; peptides; paramagnetic ions; lanthanides; MAS NMR.**

To understand how integral components of membranes such as proteins, peptides, lipids, and sterols express their diverse biological functions, it is essential to determine their structure and precise location in the membrane. Of particular interest is the polar interfacial region of membranes where many interactions between membraneous components and the extracellular or cytoplasmic environment occur. Solid state MAS NMR spectroscopy (*1, 2*) now allows one to obtain high-resolution like spectra for membrane systems which are not accessible to conventional solution NMR methodology due to their slow tumbling rates. While ^{31}P MAS NMR provides only local information for the phospholipid headgroup region close to the phosphorous nucleus (*3*), ^{13}C CP MAS NMR can provide information simultaneously for the various sites across the whole molecule (*1, 4*). For pure lipid bilayers, spectral resolution is sufficient for a complete assignment of all carbon atoms in a lipid molecule (*4*). Thus, the influence of membrane effectors, such as cholesterol, has been studied simultaneously at atomic resolution at all positions of the lipid and sterol molecules providing a comprehensive picture across the whole bilayer (*4–7*).

To probe the location of membrane compounds relative to the membrane surface, a method is presented based on a site-resolved observation of the nuclear spin-relaxation-enhancement effect through paramagnetic probes (*5, 8*), by using a combination of Dy^{3+} ions bound to dimyristoylphosphatidylcholine (DMPC) bilayers and high-resolution ^{13}C CP MAS NMR. The binding of this trivalent ion to the bilayer surface permits observation of quenching of resonances arising from the different sites of embedded molecules which are in close proximity to the polar interface or outside the membrane. The decay of intensities with titration of Dy^{3+} ions for the various carbon sites across the membrane was observed to be correlated to its distance to the bound cation. Finally, the applicability of this method to localize a membrane-bound peptide is demonstrated with the 50 residue long M13 coat protein which was specifically $^{13}C{=}O$ labeled at Val-29 and $^{13}C_{\alpha}$ labeled at Val-31. It is shown that these residues, as suggested from other studies, are deeply buried inside the membrane bilayer and therefore not effected by the binding of lanthanides to the membrane surface.

The NMR spectrum in Fig. 1a shows all ^{13}C resonances for DMPC bilayers with chemical shift values covering nearly 200 ppm. The resonance lines reflect the isotropic chemical shift values of the various carbons in the lipid molecule since no spinning sidebands were observed. Characteristic for this L_{α} lipid phase are very narrow linewidths due to the various motional processes which contribute to the low spin–spin relaxation rates (*6, 9*). The spectrum can be divided roughly into four main spectral groups, aliphatic fatty acid chains, polar headgroup, glycerol backbone, and carbonyl groups. Based on previous studies (*4, 7*), a complete, unambiguous assignment of all the resonances was possible, including even the individual resonances for the *sn*-2 and *sn*-1 carbonyl groups (173.3

[1] To whom correspondence should be addressed.

1090-7807/99 $30.00

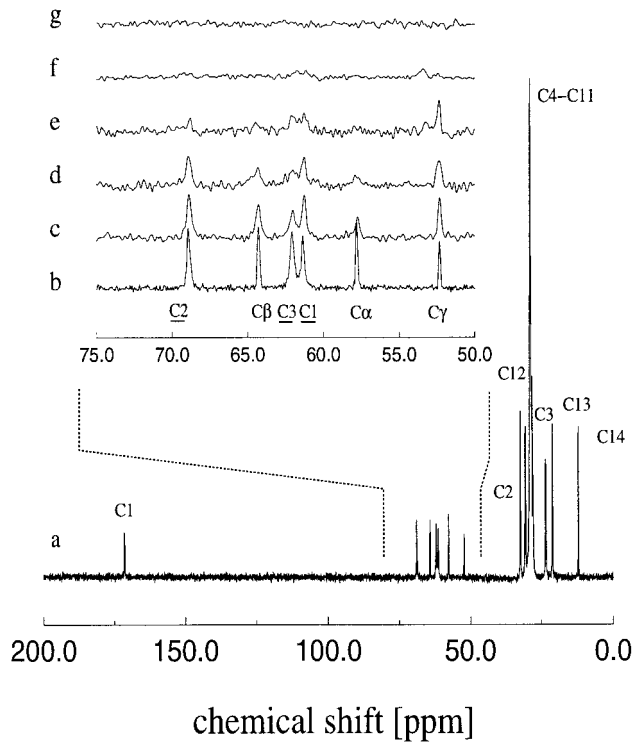

FIG. 1. (a) Proton (400.13 MHz) decoupled ^{13}C CP MAS NMR spectrum of multilamellar DMPC membranes at 308 K, 5000 Hz spinning speed and 2.5 ms CP mixing time using RAMP CP. Inset: extended spectra of the headgroup and glycerol ^{13}C resonance region without and with various concentrations of $DyCl_3$ solution: (b) 0 mM, (c) 1 mM, (d) 2 mM, (e) 5 mM, (f) 10 mM, (g) 25 mM. Atom labeling nomenclature according to (*4, 6*). Sample preparation: L-α-DMPC (Sigma, UK) dispersions prepared by adding either 60% w/w of double distilled water to 20 mg of dried lipid or appropriate aliquots of 25 mM $DyCl_3$ stock solution (Aldrich, UK). Complete homogenization for all samples was achieved by three cycles of freezing with liquid N_2 and thawing at 37°C. Membrane dispersions were pelleted into 4 mm MAS NMR rotors (Bruker, Karlsruhe, Germany), sealed, and immediately measured.

and 173.1 ppm) and both chain-C3 carbons (25.3 ppm for *sn*-2 position, 25.1 ppm for *sn*-1 position). The resonances arising from the headgroups and backbone which both occur in the region of the spectrum (50–70 ppm) are assigned as indicated in Fig. 1b. Addition of Dy^{3+} lanthanide ions (1–25 mM) to DMPC bilayers leads gradually to a loss of spectral intensity for various headgroup and backbone ^{13}C NMR resonances and finally results in a complete disappearence of these resonances at a concentration of 25 mM Dy^{3+} (Figs. 1b–1g).

In general, the interaction of paramagnetic ions with nearby nuclei can take place in two ways, by Fermi contact interaction, that is, by direct transmission of electron spin density through the bonds, and by electron–nucleus interactions (*10*). The Fermi contact is only of importance for nuclei which are directly adjacent to the paramagnetic center. Lanthanides associated with the anionic phosphate group of lipid molecules create a large contact contribution to the phosphorous signal, while in contrast protons and ^{13}C nuclei experience mainly dipolar interactions (*11*). Paramagnetic ions can be divided into two groups; those with long electron relaxation times cause extensive line broadening, while others with short electron relaxation times do not alter the T_2 relaxation time of the perturbed nucleus, but change their chemical shielding and so move their chemical shift upfield or downfield. In practice, paramagnetic ions act both as shift and as relaxation reagents and which of these effects dominate depends on the specific conditions (*12*). The dipolar contribution of the electron spin, S, to the nuclear spin–spin relaxation rates of a nucleus I assuming an isotropic g-tensor and isotropic rotational tumbling is expressed as (*12*)

$$\frac{1}{T_{2M}} = \frac{1}{15}\frac{\gamma_I^2\mu_S^2}{r_{IS}^6}\left(4\tau_C + \frac{3\tau_C}{1+\omega_I^2\tau_C^2} + \frac{13\tau_C}{1+\omega_S^2\tau_C^2}\right) \quad [1]$$

where γ_I is the magnetogyric ratio, μ_S the magnetic moment, r_{IS} is the vector between the paramagnetic ion and the observed nucleus, and ω_S and ω_I are the electronic and nuclear Larmor frequencies (with $\omega_S \gg \omega_I$). The correlation time τ_C is given by

$$\frac{1}{\tau_C} = \frac{1}{\tau_R} + \frac{1}{T_{1e}} + \frac{1}{\tau_M}, \quad [2]$$

where τ_R is the overall rotational correlation time of the observed complex, T_{1e} is the electronic spin relaxation time, and τ_M is the lifetime of the complex. For lanthanide ions, which have relatively short electron spin relaxation times of 0.1–0.4 ps, relaxation terms need to be added to the expressions above (*13*):

$$\frac{1}{T_{2M}^{\kappa}} = \frac{1}{5}\frac{\gamma_I^2 B_0^2 \mu_S^4}{(3kT)^2 r_{IS}^6}\left(4\tau_R + \frac{\tau_R}{1+\omega_I^2\tau_R^2}\right). \quad [3]$$

It can be seen that the T_2 contribution to the linewidth increases with the field strength B_0^2 and with μ_S^4. The magnetic moment of Dy^{3+} is large with a value of $10.5 \times \beta$ (β, Bohr magneton) (*14, 15*) which means it contributes significantly to the nuclear relaxation, in particular to T_2.

As seen in Fig. 1c, already at a concentration as low as 1 mM, the intensities and linewidths of all resonances between 50 and 70 ppm are affected, with the glycerol-C3 and the choline C_α resonance lines affected most. At 2 mM Dy^{3+}, the C3 and C_α resonance lines are almost completely quenched, and the other resonances show a further more significant reduction in their intensities, but with concomittant small ($\leq$0.2 ppm) chemical shift changes as expected due to the very small scalar contributions. Paramagnetic relaxation effects, i.e., T_{2M} contributions to T_2, are therefore larger than the chemical shift contribution under our experimental conditions, as pointed out and observed for small sonicated vesicles (*16*) and recently on bicelles (*15*). Since all the headgroup and backbone resonances

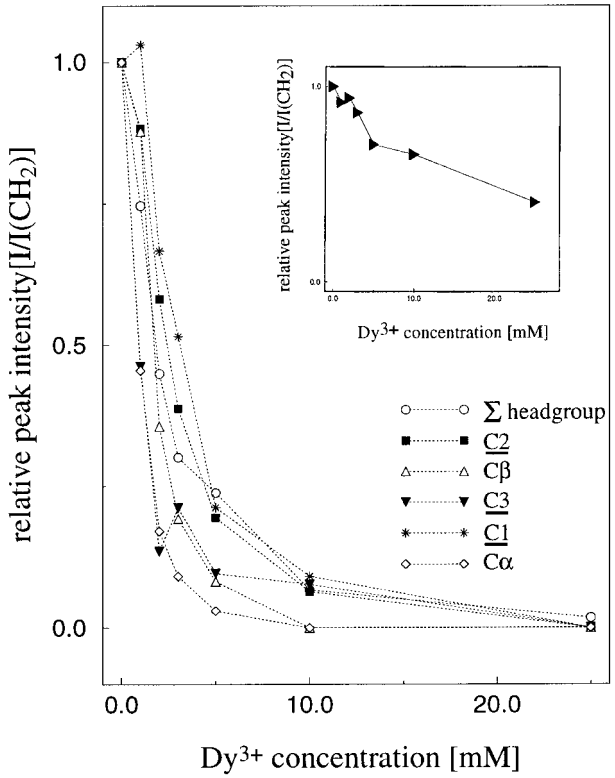

FIG. 2. Effect of Dy^{3+} added at various concentrations to the relative intensities of the headgroup and backbone ^{13}C NMR resonances of DMPC bilayers at 308 K (spectra shown in Fig. 1). Intensities expressed as fraction of the unaffected lipid fatty acid chain CH_2 groups and scaled up to 100% for the ion-free system for each resonance. Open circle: Sum of headgroup and backbone intensities. Inset diagram: relative decay of intensities for the chain-C3 resonances.

are significantly affected upon addition of only moderate levels (<2 mM) of metal ions, the lifetime of a lanthanide–lipid complex must be very short on the NMR timescale, as observed previously (*17*).

The degree of intensity loss for the various carbon atoms near the membrane surface as a function of the Dy^{3+} concentration, as monitored by the normalized integral intensity for each carbon signal as a fraction of the total fatty acid chain (C_4–C_{11}) segment resonance intensity, was plotted against the Dy^{3+} concentration (Fig. 2), with the inset displaying the decay for the chain-C3 signals. The most dramatic loss of up to 60% in spectral intensity upon addition of 1 mM Dy^{3+} occurs for the glycerol-C3 and the choline C_α atoms, while glycerol-C2 and C_β positions are only effected to about 15%. The obtained curves are, however, only semi-quantative due to the high dynamic disorder of the lipid molecules in the liquid crystalline state of the membrane (*18–20*). In this phase, the aliphatic chain segments (C_4–C_{11}) used for normalization are far enough away in their time-average motional excursions from surface localized ions. However, due to the high conformational flexibility there is a finite time probability that various chain segments will be near the interface (*20, 21*) and could experience a paramagnetic effect. Since the probability for this event is still very low (<10% (*21*)) the related NMR resonances are still much less effected than carbons at the interface. However, this effect is observable, especially at higher concentrations (>5 mM) resulting in only a semi-quantitative plot.

Analyzing the different decay curves in Fig. 2 permits the binding site for the Dy^{3+} to be described. These effects are most pronounced for the carbon atoms C3 and C_α, which are the direct neighbors of the PO_4^- group, indicating that Dy^{3+} binds to this charged group, a conclusion which has been made previously (*16, 22*). The decay in intensities for the C_β and C2 carbons are less pronounced, an indication of a more remote distance (with a r_{IS}^{-6} dependence) to the lanthanide binding site. To correlate the observed intensity decays with structural information regarding distances between the lanthanide binding site and a specific carbon site, it is necessary to encount for the fluid-phase nature of the lipid bilayer (*18, 20, 21*), also explained above. Therefore the probability of finding a structural lipid group at a particular transbilayer location in time-average is used to correlate the relevant distances of the glycerol backbone, chain C2 and C3 carbon sites to the intensity of paramagnetic quenching as shown in Fig. 3 at the presence of 5 mM Dy^{3+}. A good correlation between relative distance to the membrane surface and the decay of relevant intensities is observed, a correlation which permits the time-averaged distances of different carbons to the membrane surface for other membrane compounds such as peptides or anesthetics, whose location in the membranes are yet unknown, to be deduced.

Using the 50 residue long M13 coat protein incorporated into DMPC bilayers at a molar lipid to protein ratio of 30:1, the positions of two specifically ^{13}C labeled protein residues in the membrane were located using Dy^{3+} quenching methods. The

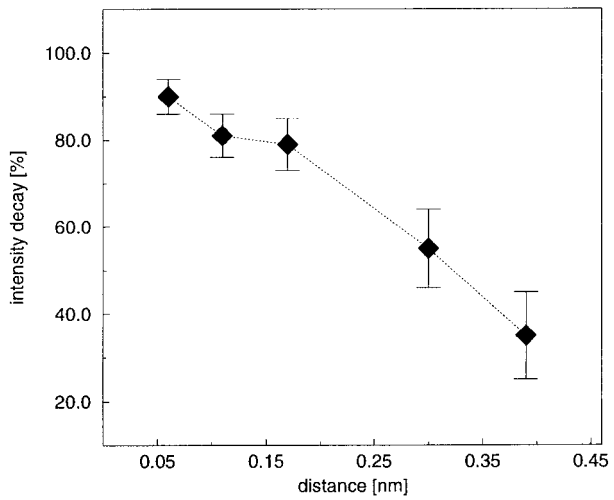

FIG. 3. Distance dependent effect of 5 mM Dy^{3+} on resonance intensities of various carbon atoms of the lipid backbone and upper chain part of DMPC at 308 K. Plotted are the normalized intensity decays (maximal 100%) against the average distance of various carbon sites (see text for details).

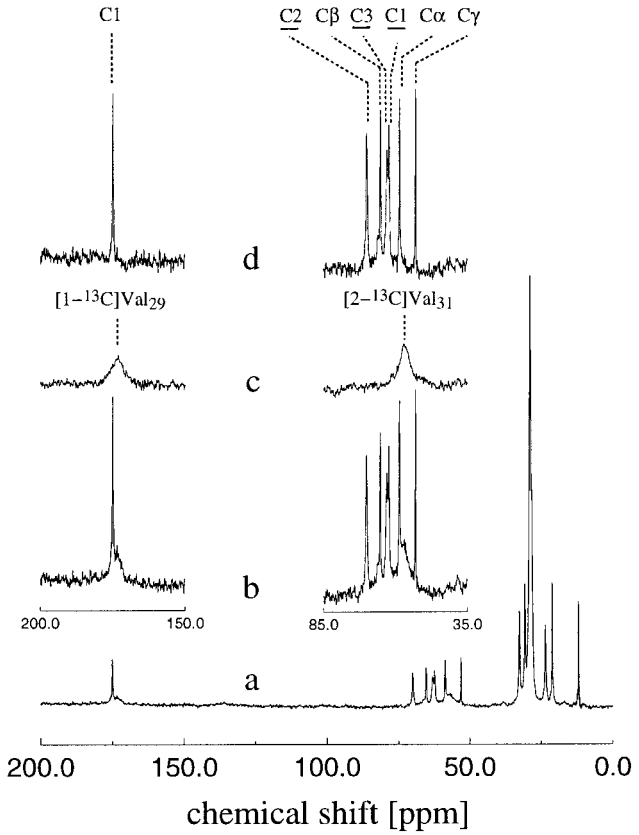

FIG. 4. Proton (200.13 MHz) decoupled ^{13}C CP MAS spectra of multilamellar DMPC membranes containing M13 coat protein at a molar lipid to protein ratio of 30:1 before and upon adding of 10 mM $DyCl_3$ solution at 308 K: (a) full spectrum of lanthanide-free M13/DMPC complex. (b) Extended regions of (a) from carbonyl peaks (left) and headgroup, glycerol lipid peaks and C_α protein peaks (right). (c) Same extended regions as in (b) but after addition of 10 mM Dy^{3+}. (d) Spectra obtained for the same regions after subtraction of spectra of treated complexes (c) from lanthanide-free (b). Experimental conditions: 308 K, 1900 Hz spinning speed, 2.5 ms CP mixing time, and 100,000 scans each. Sample preparation: M13 coat protein ($^{13}C{=}O$ labeled at Val-29, $^{13}C_\alpha$ labeled at Val-31, Asp-5 replaced by Asn) was synthesized using standard solid-phase FMOC chemistry (NSR Centre, Nijmegen, Netherlands). The purity of the protein was checked by HPLC and MS and found to be over 90%. Incorporation of M13 coat protein into DMPC bilayers at 30:1 lipid to protein ratio was carried out, adapted from a method described earlier (*26*). Incorporation of the protein in an α-helical form was checked by CD-measurements (Jasco, USA). Finally the sample was resuspended either in water or appropriate Dy^{3+} solution at the same pH and pelleted into 7 mm MAS NMR rotors.

protein was $^{13}C{=}O$ labeled at Val-29 and $^{13}C_\alpha$ labeled at Val-31 in its transmembrane region. ^{13}C CP MAS NMR experiments were performed on multilamellar DMPC/M13 vesicles before and upon addition of 10 mM aqueous Dy^{3+} solution at 308 K and 1.9 kHz spinning speed. Figure 4a shows the ^{13}C NMR spectrum for the peptide–lipid bilayers using the same chemical shift range as in Fig. 1a. As expected, the spectrum is very similar to the one for peptide-free DMPC bilayers except for two additional broad resonances at 170 and 56 ppm arising from the labeled protein residues. Figure 4b shows the expanded spectral regions where the ^{13}C resonances of both Val residues in the protein appear as two resonances. The narrow sharp resonance line at 171.8 ppm can be assigned to the lipid carbonyl groups. The second, very broad resonance at 170 ppm indicates the carbonyl group of the Val-29 residue. The expanded spectrum showing the 35–85 ppm chemical shift region in Fig. 4b reveals all the expected resonances for the lipid backbone and headgroup carbons. Additionally a new broad resonance, similar to the one at 170 ppm, appears at 56 ppm and is assigned to the $^{13}C_\alpha$ carbon in the Val-31 residue. Since both residues show the same inhomogeneous line broadening and CP profile behavior, it can be assumed that for the transmembrane helical part of the peptide, a certain distribution of conformational states exists with a highly restricted dynamics, an observation in agreement with other recent studies (*23, 24*).

Upon addition of 10 mM Dy^{3+} solution to the M13/DMPC vesicles all ^{13}C signals arising from the lipid carbons are undetectable in the expanded spectral regions (Fig. 4c) as seen previously for peptide-free bilayers (Fig. 1f). However, both protein resonances are still fully visible and apparently unaffected by the presence of trivalent ions. To determine now any ion induced effect on these resonance lines, a quantitative analysis was carried out. Additionally the spectrum for the lanthanide-treated system was substracted from the spectrum of the lanthanide-free system. The results (Fig. 4d) show only lipid resonances and clearly demonstrate that neither a change in the linewidths nor a drop in absolute intensity for these protein resonances occur upon addition of 10 mM Dy^{3+} solution. This finding indicates that both Val-29 and Val-31 residues are necessarily located inside the hydrophobic part of the lipid bilayer remote from the Dy^{3+}–lipid binding site, a conclusion which confirms earlier studies showing both residues as part of the membrane spanning region of the protein (*24, 25*). This transmembrane sequence has an α-helical structure in the reconstituted DMPC/M13 bilayer, in agreement with earlier studies (*26*) and mimics the *in vivo* state in the plasma membrane (*25*). Since the chain-C3 resonances of the DMPC lipids are still affected by the binding of Dy^{3+}, it is assumed that Val-29 and Val-31 are situated below this position in the membrane. In general our method presents a simple direct way to obtain information about the location of labeled proteins in membranes by MAS NMR without the inherent disadvantage of other techniques which mainly use modified systems including bulky reporter molecules (*27, 28*) except neutron scattering studies on oriented systems (*29*).

ACKNOWLEDGMENTS

Financial support from BBSRC (43/B04750) and the EU (TMR Contract FMRX-CT96-0004) is gratefully acknowledged. C.G. was the recipient of a C. Rhodes Scholarship and A.W. of a BBSRC Senior Fellowship. We are very grateful to C. Wolfs for his help with M13 protein reconstitution and E. Mitchell and P. Fisher for all general help.

REFERENCES

1. S. O. Smith, K. Aschheim, and M. Groesbeek, Magic angle spinning NMR spectroscopy of membrane proteins, *Q. Rev. Biophys.* **29,** 395–449 (1996).
2. A. Watts, A. S. Ulrich, and D. A. Middleton, Membrane protein structure: The contribution and potential of novel solid state NMR approaches (review), *Mol. Membr. Biol.* **12,** 233–246 (1995).
3. T. J. T. Pinheiro and A. Watts, Resolution of individual lipids in mixed phospholipid membranes and specific lipid-cytochrome C interactions by magic-angle spinning solid-state phosphorus-31 NMR, *Biochemistry* **33,** 2459–2467 (1994).
4. J. Forbes, J. Bowers, X. Shan, L. Moran, E. Oldfield, and M. A. Moscarello, Some new developments in solid-state nuclear magnetic-resonance spectroscopic studies of lipids and biological-membranes, including the effects of cholesterol in model and natural systems, *Faraday Trans. I* **84,** 3821–3849 (1988).
5. J. Villalain, Location of cholesterol in model membranes by magic-angle-sample-spinning NMR, *Eur. J. Biochem.* **241,** 586–593 (1996).
6. C. Le Guerneve and M. Auger, New approach to study fast and slow motions in lipid bilayers-application to dimyristoylphosphatidylcholine-cholesterol interactions, *Biophys. J.* **68,** 1952–1959 (1995).
7. W. Guo and J. A. Hamilton, A multinuclear solid-state NMR study of phospholipid-cholesterol interactions. Dipalmitoylphosphatidylcholine–cholesterol binary system, *Biochemistry* **33,** 14174–14184 (1995).
8. G. D. Henry and B. D. Sykes, Methods to study membrane protein structure in solution, *Methods Enzymol.* **239,** 515–535 (1994).
9. K. Weisz, G. Gröbner, C. Mayer, J. Stohrer, and G. Kothe, Deuteron nuclear magnetic resonance study for the dynamic organization of phospholipid/cholesterol bilayer membranes: Molecular properties and viscoelastic behavior, *Biochemistry* **33,** 1100–1112 (1992).
10. C. N. La Mar, W. Horrocks, and R. H. Holms, "NMR of Paramagnetic Molecules," Academic Press, New York (1973).
11. L. D. Bergelson *in* "Paramagnetic Hydrophilic Probes in NMR Investigations of Membrane Systems," pp. 275–331, Plenum Press, New York (1978).
12. R. A. Dwek, "Nuclear Magnetic Resonance in Biochemistry," Clarendon Press, Oxford (1973).
13. A. J. Vega and D. Fiat, Nuclear relaxation processes of paramagnetic complexes. The slow-motion case, *Mol. Phys.* **31,** 347–351 (1976).
14. B. Bleaney, Nuclear magnetic resonance shifts in solution due to lanthanide ions, *J. Magn. Reson.* **8,** 91–100 (1972).
15. R. S. Prosser, J. S. Hwang, and R. R. Vold, Magnetically aligned phospholipid bilayers with positive ordering: A new model membrane system, *Biophys. J.* **74,** 2405–2418 (1998).
16. H. Hauser, M. C. Phillips, B. A. Levine, and R. J. B. Williams, Ion-binding to phospholipids, *Eur. J. Biochem.* **58,** 133–144 (1975).
17. Y. K. Levine, A. G. Lee, N. J. M. Birdsall, J. C. Metcalfe, and J. D. Robinson, The interaction of paramagnetic ions and spin labels with lecithin bilayers, *BBA* **291,** 592–607 (1973).
18. A. J. Robinson, W. G. Richards, P. J. Thomas, and M. M. Hann, Head group and chain behavior in biological membranes: A molecular dynamics computer simulation, *Biophys. J.* **67,** 2345–2354 (1994).
19. R. L. Thurmond, G. Lindblom, and M. F. Brown, Curvature, order, and dynamics of lipid hexagonal phases studied by deuterium NMR spectroscopy, *Biochemistry* **32,** 5394–5410 (1993).
20. W.-M. Yau, W. C. Wimley, K. Gawrisch, and S. H. White, The preference of tryptophan for membrane interfaces, *Biochemistry* **37,** 14713–14718 (1998).
21. D. Huster and K. Gawrisch, NOESY NMR crosspeaks between lipid headgroups and hydrocarbon chains: Spin diffusion or molecular disorder? *JACS* **121,** 1992–1993 (1999).
22. H. Akutsu and J. Seelig, Interaction of metal ions with phosphatidylcholine bilayer membranes, *Biochemistry* **20,** 7366–7373 (1981).
23. C. H. M. Papavoine, M. L. Remerowski, L. M. Horstink, R. N. H. Konings, C. W. Hilbers, and F. J. M. Van de Ven, Backbone dynamics of the major coat protein of bacteriophage M13 in detergent micells by 15N nuclear magnetic resonance relaxation measurements using the model-free approach and reduced spectral density mapping, *Biochemistry* **36,** 4015–4026 (1997).
24. P. A. McDonnell, L. Shon, Y. Kim, and S. J. Opella, fd coat protein-structure in membrane environments, *J. Mol. Biol.* **233,** 447–463 (1993).
25. D. A. Marvin, Filamentous phage structure, infection and assembly, *Curr. Opin. Struct. Biol.* **8,** 150–158 (1998).
26. R. B. Spruijt, J. A. M. Wolfs, and M. A. Hemminga, Aggregation-related conformational change of the membrane-associated coat protein of bacteriophage M13, *Biochemistry* **28,** 9158–9165 (1989).
27. K. A. Jansen, T. Pali, D. Marsh, D. Stopar, and M. A. Hemminga, Membrane location of spin-labeled M13 major coat protein mutants determined by paramagnetic relaxation agents, *Biochemistry* **36,** 8261–8268 (1997).
28. R. D. Kaiser and E. London, Location of diphenylhexatriene (DPH) and its derivatives within the membranes: Comparison of different fluorescence quenching analysis of membrane depth, *Biochemistry* **37,** 8180–8190 (1998).
29. J. P. Bradshaw, C. E. Dempsey, and A. Watts, A combined X-ray and neutron diffraction study of selectively deuterated melittin in phospholipid bilayers: Effect of pH, *Mol. Membr. Biol.* **11,** 79–86 (1994).